Toxicology Reports 5 (2018) 333–342

Contents lists available at ScienceDirect

Toxicology Reports

journal homepage: www.elsevier.com/locate/toxrep

Phytofabrication of Silver nanoparticles: Novel Drug to overcome hepatocellular ailments

Asha Singh[a,*], Mohd Yaqoob Dar[b], Beenu Joshi[c], Bhawna Sharma[c], Sadhana Shrivastava[a], Sangeeta Shukla[a,*]

[a] UNESCO- Trace Element Satellite Centre, School of Studies in Zoology, Jiwaji University, Gwalior, M.P., India
[b] Department of Natural Sciences, SBBS University, Jalandhar, Punjab, India
[c] Department of Immunology, National JALMA Institute for Leprosy and Other Mycobacterial Diseases, Agra, U.P., India

ARTICLE INFO

Keywords:
Morus alba
Silver nanoparticles
N-Nitrosodiethylamine
HepG2
Liver

ABSTRACT

This study aimed to treat hepatocellular ailments with biologically prepared silver nanoparticle (AgNPs). AgNPs were formulated using *Morus alba* leaf extract and their synthesis and characterization were determined by UV–visible spectroscopy, Transmission Electron Microscope (TEM), Scanning Electron microscope (SEM), X-ray diffraction (XRD), Fourier transform infrared spectroscopy (FT-IR) and Zeta analysis. *In vitro* studies on HepG2 cell lines for cytotoxic effect and *in vivo* studies in a rat model for hepatoprotective effect were carried out using biologically prepared AgNPs as curing agents. Dose response cytotoxicity on hepatic cancer (HepG2) cells was confirmed by 3-(4, 5-dimethyl thiazole-2-yl)-2, 5-diphenyl tetrazolium (MTT) assay. The inhibitory concentrations (IC_{50}) were found to be 20 µg/mL and 80 µg/mL for AgNPs and *M. alba* leaf extract respectively against HepG2 cells at 24 h incubation. In addition, hepatotoxicity in Wistar rats (180 ± 10 g) was induced by intraperitoneal injection of *N*-nitrosodiethylamine (NDEA) and were treated with different doses of AgNPs (25, 50, 100 µg/kg). NDEA administration showed a significant rise in the biochemical parameters whereas the levels of enzymic antioxidants were decreased. Obtained results revealed that the elevated levels of Liver Function Test (LFTs) biomarkers were significantly reversed and the antioxidant levels were significantly recouped towards normal after the conjoint treatment of AgNPs in a dose-dependent manner. Thus green synthesized AgNPs showed a promising curing effect on hepatocellular ailments.

1. Introduction

Nanotechnology has played a crucial role and is the most proficient technology that can be functional in the fields of pharmaceutical, healthcare, biomedical and drug delivery [1,2]. Nanoscale particles are developed for use in drug delivery because they increase the drug dissolution rate, leading to enhanced drug absorption and bioavailability [3–5]. Silver nanoparticles possess electrical, optical as well as biological properties and are thus applied in biosensing, imaging, drug delivery, nanodevice fabrication and in medicine [6]. Various physicochemical properties such as low solubility or high lipophilicity were the foremost inevitable problems faced by the pharmaceutical industry in the development of a pharmacologically active substance with relevant activity and minimum toxicity [7]. Hence, various techniques are used for the improvement of the solubility of poorly soluble drugs. The metallic nanoparticles are used as valuable tools to enhance the effectiveness of the current therapies and to increase the compliances of the patient to the treatments. Thus finding a proper method to obtain a nanoparticle with a reduced number of inconveniences related to the physio-chemical properties of the nanoparticles, in terms of stability, biocompatibility, the proper size, and shape for biochemical uses, represented a real challenge for the researchers [8]. Transport of nanoparticles through the extracellular matrix (ECM) is complicated due to its mesh-like organization and the particles with a size larger than the network space are rejected by ECM, while smaller particles are able to pass through the matrix barrier [9,10].

Synthesis of AgNPs with the help of biological agents is more eco-friendly, cost-effective and highly focused research area compared to other chemical and physical methods due to reduced use of hazardous reagents and solvents, improved material and energy efficacy from the chemical process and enhanced design of nontoxic products [11,12]. The uses of plant extract for nanoparticles synthesis proved to be advantageous than microbiological processes, because pathogenic bacteria may contaminate the nanoparticles when used in biomedical fields

* Corresponding authors at: Reproductive Biology and Toxicology Laboratory, UNESCO- Trace Element Satellite Centre, School of Studies in Zoology, Jiwaji University, Gwalior, M.P., 474011, India.
E-mail addresses: ashasgh87@gmail.com (A. Singh), profsshukla@gmail.com (S. Shukla).

https://doi.org/10.1016/j.toxrep.2018.02.013
Received 16 June 2017; Received in revised form 27 February 2018; Accepted 27 February 2018
Available online 01 March 2018

[13].

Green synthesized silver nanoparticles are essential in medical applications because of appealing features such as the use of natural resources, rapidness, eco-friendliness, and benignancy. Such nanoparticles are devoid of contaminants and the process is easy to scale-up [14]. It is one of the best methods for the production of nanoparticles because it involves the plant extract as capping and reducing agent due to their reducing properties [15]. Various plant extracts *viz.*, *Ficus religiosa*, *Gymnema sylvestre, Embilica Officinalis, Moringa oleifera, Phyllanthus emblica, Melia azedarach, Annona squamosa, Andrographis paniculata, Cinnamon zeylanicum* were reported in literature with ability to develop nanoparticles as nano drug to treat medical implication [16–21] Aqueous leaf extract of *Azadirachta indica* has been found to be suitable reducing and caping agent for the synthesis of silver nanoparticles [22]. In this regard, leaf extract of *Morus alba* (mulberry) a species of family Moraceae, was used for fabrication of silver ion to nanoparticles. It is a deciduous tree that is widely distributed in Asia. All parts of this tree such as leaves, fruits, and roots have been used in traditional medicine [23]. *Morus alba* leaf contains triterpenes (lupeol) Sterols (β-Sitosterol), bioflavonoids (rutin, moracetin, quercetin-3-triglucoside and isoquercitrin), coumarins, volatile oil, alkaloids, amino acids and organic acids [24].

Hepatocarcinogenesis is one of the most common malignancies worldwide and the fourth most common causes of cancer mortality in Asia [25]. The conventional therapy for liver cancer including chemotherapy, radiation, surgical resection, and ablation gives little hope for the restoration of health because of poor diagnosis and serious side effects. Many challenges remain in treating cancer patients, including treatment-related adverse effects, poor outcomes, lack of a therapeutic target and balancing treatment toxicity with the quality of life in patients with metastatic cancer who have already received extensive therapy. Therefore, there is still an urgent need for new therapeutic options for cancer [26]. *N*-nitrosodiethylamine (NDEA), N-nitroso alkyl compound, is a potent hepatotoxin present in wide variety of foods such as cheese, soybean, smoked, salted and dried fish, cured meat and alcoholic beverages they are formed by the reaction of amines and amides with nitrosating agents derived from nitrite [27,28]. It is presumptive that NOCs formed endogenously in the stomach or intestines after consumption of nitrite-preserved foods like processed meat or fish and are absorbed into the bloodstream and reach the brain [29].

NDEA induced hepatocellular carcinoma (HCC) is considered as one of the most accepted and widely used experimental models to study hepatocarcinogenesis in rats [30]. NDEA metabolism in the liver by cytochrome isoform 2E1 (CYP 2E1) generates reactive oxygen species (ROS) causing oxidative stress [31] and oxidative damage leading to cytotoxicity, carcinogenicity, and mutagenicity [32].

A lot of work has been done on medicinal implications of AgNPs, but to the best of our knowledge, this is the first ever piece of work considering the two aspects. The first aspect is with regard to synthesis of AgNPs using *M. alba* leaf extract. The second important aspect was to evaluate the therapeutic efficiency of biosynthesized AgNPs against NDEA induced hepatocellular ailments in a rat model and reflect their cytotoxicity against *in vitro* HepG2 cells.

2. Materials and methods

2.1. Chemicals and reagents

N-Nitrosodiethylamine (PubChem CID: 5921), Silver nitrate (PubChem CID: 24470), Silymarin (PubChem CID: 5213), Dulbecco's Modified Eagle's Medium (DMEM), fetal bovine serum (FBS), glutamine (PubChem CID: 5961), penicillin and streptomycin (PubChem CID: 86591708), were purchased from Sigma-Aldrich Chemical Company (USA). Trypan blue (PubChem CID: 9562061) and MTT [3-(4, 5- dimethyl thiazol-2-yl)-2, 5-diphenyl tetrazolium] dye (PubChem CID: 64965) and 5-fluorouracil (5-FU) (PubChem CID: 3385) were obtained from Himedia laboratories (Mumbai, MH, India). Rest of the other chemicals, as well as solvents utilized, were of high purity in addition to analytical class sold by, E- Merck (Germany), Ranbaxy Pvt. Ltd. Company (India).

2.2. Preparation of aqueous leaf extract

Leaves of mulberry were collected from the maintained plants at CSR & TI, Central Silk Board, Pampore, Jammu and Kashmir, India, were identified by Dr. A.K. Jain, Director Institute of Ethnobiology, Jiwaji University Gwalior and were stored in same Institute under Voucher specimen No. 326. Leaves were rinsed thoroughly with tap water followed by distilled water to remove all the dust and unwanted visible particles. The leaves were shade dried at room temperature for 2–3 weeks and then powdered. About 10 g of leaf powder was added to 100 ml of sterile distilled water in a 250-ml Erlenmeyer flask and this mixture was boiled in a water bath at 60 °C for 1–2 h. After cooling to room temperature, the mixture was filtered by using muslin filter cloth. The filtrate was further filtered through 0.6 µm sized filters and then stored in an airtight container at +4 °C for further experiments.

2.3. Fabrication of AgNPs

An aqueous solution (1 mM) of silver nitrate ($AgNO_3$) was prepared and used for the synthesis of AgNPs. The preparation of AgNPs was carried out by adding 5 ml of aqueous leaf extract to 95 ml of $AgNO_3$ solution in 250 ml Erlenmeyer flasks and kept in a rotary shaker (Remi elektrotechnik limited) at a different temperature such as 30 °C, 60 °C, 90 °C and 95 °C. The reaction mixture was monitored spectrophotometrically after incubation of 60 min. Reduction of silver nanoparticles was observed by a color change in the reaction mixture during temperature treatments. Complete reduction of $AgNO_3$ to Ag^+ ions and their restoration to metallic silver (nanoparticles) was confirmed by the change in color from light yellow to colloidal brown. The reactions were carried out in dark to avoid photoactivation of $AgNO_3$. After irradiation, the colloidal mixture was purified by centrifugation at 10,000 rpm for 10 min at 4 °C followed by redispersion of the pellet in Milli-Q water and dried in a vacuum distillation; powder form of fabricated AgNPs was weighed, sealed and stored in the dark at 4 °C [33].

2.4. Characterization of AgNPs

The alteration of color from yellowish to dark brown in the colloidal mixture was measured as an initial remark for the breakdown of silver nitrate. Suspension of samples (1 ml) were collected at regular increasing temperature to observe the completion of bioreduction of Ag^+ in aqueous solution, followed by dilution of the samples with 2 ml of deionized water and subsequently scanned in UV–vis spectra, flanked by 200–800 nm wavelengths by spectrophotometer (UV 3000$^+$ LABINDIA), having a resolution of 0.5 nm. The presence of functional biomolecules in *M. alba* mediated AgNPs were confirmed by FT-IR spectrometry (Perkin-Elmer, AD-6 Waltham, MA, USA). Transmission Electron Microscopy (FEI's Tecnai™ G2) was used to envisage the morphology and size of the AgNPs. Grids of TEM were organized by putting a 5 µl of the AgNP solutions on carbon-coated copper grids as well as dried beneath the lamp. The surface analysis of the synthesized AgNPs was studied using scanning electron microscope (SEM). The SEM images were recorded (Zeiss EVO 18, Germany) at 40,000 × magnifications operating with 20.00 kV. The crystal lattice of the synthesized NPs was determined by XRD measurements using an XRD-6000 X-ray diffractometer (Shimadzu, Kyoto, Japan). To study the zeta potential stability of the nanoparticles Malvern Zetasizer Nano series compact scattering spectrometer (Nano ZS 90, Malvern Instruments Ltd., Malvern U.K.) was used.

2.5. Cell maintenance and culture procedures

The hepatocellular carcinoma cell lines (HepG2) were purchased from the National Centre for Cell Sciences, Pune, India. The HepG2 cells were cultured under standard conditions in Dulbecco's Modified Eagle Medium (DMEM), supplemented with antibiotic-antimycotic solution, L-glutamine (2 mM) and 10% heat-inactivated fetal bovine serum (FBS) in a humidified CO_2 incubator at 37 °C. The stock solutions of AgNPs and *M. alba* extract were prepared in culture medium (without FBS) and filtered through 0.2-μm syringe filters and stored at 4 °C. Further, working dilutions were made in culture media to obtain the desired concentration. 5-Fluorouracil (5-FU) a known anticancer agent was used as a control in each experiment.

2.6. Trypan blue exclusion test

Viability and purity of cells were estimated by trypan blue exclusion test. After trypsinization cells were suspended medium supplemented with 10% heat-inactivated FBS. 10 μl cells from cell suspension were diluted in 1:10 dilution with 0.4% trypan blue solution, 10 μl of this dilution was loaded on Neubauer's chamber and cells were counted under a phase contrast microscope and the number of viable cells was calculated. Viability was expressed as a percentage of control number of cells excluding trypan blue dye.

2.7. MTT [3-(4, 5-dimethyl-thiazol-2yl)-2, 5-diphenyl tetrazolium bromide] assay

MTT assay based on the mitochondrial enzyme degradation of tetrazolium dye to verify cell viability [34]. Briefly, the cells were plated at a density of 8.5×10^4 cells/well into 96 well plates and allowed to adhere for 24 h in humidified CO_2 incubator at 37 °C. After incubation cells were treated with different concentrations of test samples and volume was made 200 μl per well by adding medium supplemented with heat-inactivated FBS. The plate was further incubated for 24 h in humidified CO_2 incubator at 37 °C. After incubation 10 μl of MTT solution at a concentration of 5 mg/mL was added to each well and cells were incubated in humidified CO_2 incubator at 37 °C for 3–4 h in the dark until purple formazan was visible. After incubation, 100 μl of Dimethyl sulfoxide (DMSO) was added per well to dissolve purple formazan crystals and the plate was incubated in dark for 10–20 min. The absorbance was read at 570 nm using ELISA reader (Spectra Max–M2, USA). The average values were determined from triplicate. Percent inhibition was calculated by using the formula: $(C-T)/C \times 100$, where C = Absorbance of control, T = Absorbance of treatment. The IC_{50} values of test compound were compared with a standard drug.

2.8. Animals

Male albino rats of *Wistar* strain (180 ± 20 g body weight) were procured from Defence Research Department Establishment, Gwalior (M.P.) India. The rats were placed in a group of six rats per cage under standard environmental conditions (25 °C ± 2 °C and relative humidity 50% ± 5%) with alternating dark and light cycle of 12 h each. The animals were maintained on standard pellets food and water *ad libitum* for 2 weeks, in order to acclimatize them to laboratory environment before the experimentation. Guidelines for breeding and experiments on animals, 1998 defined by the Ministry of Social Justice and Empowerment of India were followed (1854/GO/Re/S/16/CPCSEA). The "Principles of Laboratory Animal Care" were adhered to, during the entire study.

2.9. Experimental design

The animals were administered NDEA at a dose of 70 mg/kg, (*intraperitoneal injection*) in normal saline (0.9%) once in a week for 21 days [35]. Conjoint treatments of synthesized AgNPs were given after 24 h of toxicant administration for 21 days. A standard known hepatoprotective drug, Silymarin (50 mg/kg, *p.o.*) was used as positive control in experiment [36]. Forty-two adult male rats were divided into seven groups (6 rats/group) as follows.

Group 1 Control (vehicle only).
Group 2 AgNPs *per se* (100 μg/kg, *p.o.*)
Group 3 NDEA (70 mg/kg, *i.p.)* once in a week for 21 days.
Group 4–6 NDEA (as in group 3) + AgNPs (25, 50, 100 μg/kg, *p.o.*)
Group 7 NDEA (as in group 3) + Silymarin (50 mg/ kg, *p.o.*)

All animals were euthanized after 24 h of last treatment and various blood and hepatic tissues biochemical parameters were performed.

2.10. Determination of LFTs biomarkers

The extent of hepatic alteration was ensured by liver function test biomarkers, *viz.* ALT, ALP, γ-GT, Albumin and total bilirubin in serum. All parameters were determined by using coral clinical commercially available kits (Coral Clinical System, Tulip Diagnostics (P) Ltd. Goa, India).

2.11. Assessment of antioxidant status in hepatic tissues

Reduced (GSH) and Oxidized glutathione (GSSG) level were determined by *O*-phthaldehyde [37]. The activities of adenosine triphosphatase (ATPase) [38] and glucose-6-phosphatase (G-6-Pase) [39] were also determined.

2.12. Histopathological examination

Hepatic tissue was collected fixed in (10%) buffered formalin and paraffin sections were primed with 5 μm thickness using microtome HM- 360. Slides were prepared and stained with hematoxylin along with eosin using autostainer XL model no N-1263. The pathological changes were examined under Leica DM LB microscope and the images were captured by Leica digital camera DC 500 attached to it with Qwin V3 software.

2.13. Statistical analysis

DATA were statistically analyzed by one-way analysis of variance (ANOVA) and means were compared by Duncan's multiple range test (DMRT) using Sigma Plot 12® software. Values were expressed as a mean ± standard error. P *value* < 0.05 was considered statistically significant.

3. Results

3.1. Confirmation of biosynthesis of AgNPs

Biological reduction of silver nitrate is one of the widely used methods for the synthesis of silver nanoparticles. The appearance of a dark brown color is the indication of the formation of silver nanoparticles. In this study color intensity increased proportionately from yellowish to dark brown at different temperature 30 °C, 60 °C, 90 °C, and 95 °C. The intense brown color was developed after one-hour incubation at a temperature of 90 °C (Fig. 1A).

3.2. Characterization of AgNPs

Under UV–vis spectrophotometric analysis, AgNPs showed characteristic, spectral band peaks at different temperatures (pH 7.0) with the significant synthesis of AgNPs at 90 °C temperature which was confirmed with UV–visible spectra showing absorbance peak of 410 nm (Fig. 1B). The presence of the dark brown color and the peak at 410 nm implies the synthesis of AgNPs. The pH 7.0 showed suitable

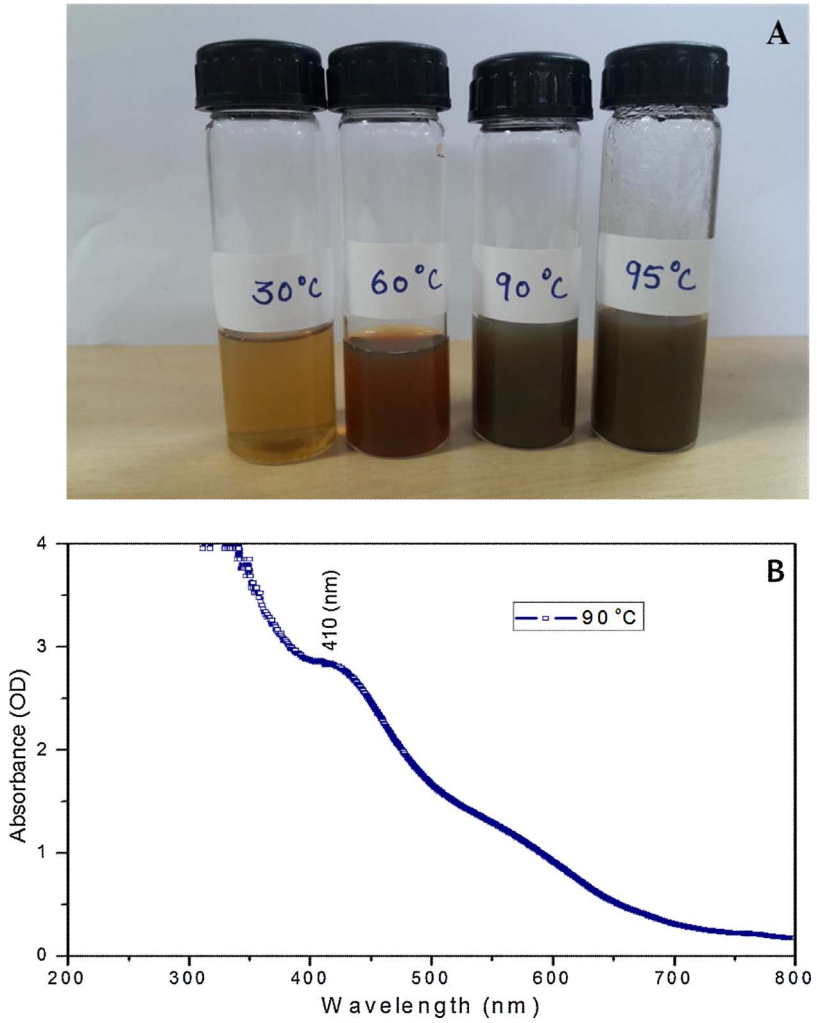

Fig. 1. Synthesis of silver nanoparticles under different range of temperatures (30 °C, 60 °C, 90 °C and 95 °C). **(A)** Colour change profile of hydrosol **(B)** UV–vis absorption spectrum of AgNPs.

environment for the creation of silver nanoparticles, hence it was used for further studies. Transmission electron microscopy (TEM) was used to identify the morphology of nanoparticles. TEM micrograph revealed well distributed spherical shaped AgNPs with an average size ranging from 10 to 50 nm (Fig. 2A). The scanning electron microscopic (SEM) analysis also showed the presence of a spherical structure of AgNPs and a similar trend was observed in the SEM micrograph (Fig. 2B). The zeta potential analysis revealed the negative charge, −11.3 mV of bio-synthesized AgNPs, indicating that the particles were scattered in the medium and are stable (Fig. 3). The large negative potential value could be due to the capping of polyphenolic constituents present in the leaf extract of *M. alba.* FT-IR analysis provided spectrum bands, incidental at 3257 cm^{-1}, 2925 cm^{-1}, 2855 cm^{-1}, 1742 cm^{-1}, 1633 cm^{-1} and 1051 cm^{-1} which represents the various functional group like O—H stretching of alcohols and phenols, N—H group (amino acids), C—O of carboxylic anions, O—H compounds (carboxylic acid), saturated C—O group and N—O stretching respectively (Fig. 4A). The absorption peak at 3257 cm $^{-1}$ indicates the presence of phenols (O—H group) and the presence of a phenolic compound in the *M. alba* were might be bind to AgNPs and were actively functional for the synthesis of nanoscale particles. The XRD pattern of the synthesized AgNPs was shown in Fig. 4B, which clearly showed crystalline nature of the AgNPs. The diffraction peak at $2\theta = 38^{\circ}$ and subsequent higher order reflections can be indexed to the Ag (678) nanoparticles. The XRD spectrum also reveals a weak peak around $2\theta = 29^{\circ}$, which can be attributed to the phytochemical components from the plant extract.

3.3. In vitro assessment of biosynthesized AgNPs cytotoxicity

Effect of biosynthesized AgNPs on cell proliferation was determined by MTT assay. The proliferation of HepG2 cells was significantly inhibited by AgNPs after 24 h incubation. The changes in the cell viability percentage in case of Control, *M. alba* and AgNPs treated HepG2 cells with different concentrations of each treatment (1, 5, 10, 20, 40 and 80 μg/mL) were presented in Fig. 5. The dose-dependent cytotoxicity was observed in AgNPs and *M. alba* treated HepG2 cells were 50% cell death, which determines the inhibitory concentration (IC_{50}) was noticed at 20 μg/mL and 80 μg/mL respectively in 24 h incubation. The cytotoxic effect was also compared with the standard anticancer drug 5-Fluorouracil (5-FU) against HepG2 cells. AgNPs showed nearly a same trend in recovery as that of standard drug (Fig. 5). The *in vitro* results showed a significant antiproliferative effect of AgNPs. On the basis of these consequences, we screened the different doses of AgNPs in *in vivo* studies.

3.4. Liver function test biomarkers

The administration of NDEA resulted in a significant increase in serum ALT, ALP, γ-GT, bilirubin with a concomitant reduction in albumin level, respectively as compared to the control group. Therapy of *M. alba* mediated AgNPs at different doses exhibit significant restoration in above indices towards normal when compared with NDEA intoxicated group ($P \leq 0.05$) (Table 1). All the doses were effective in a

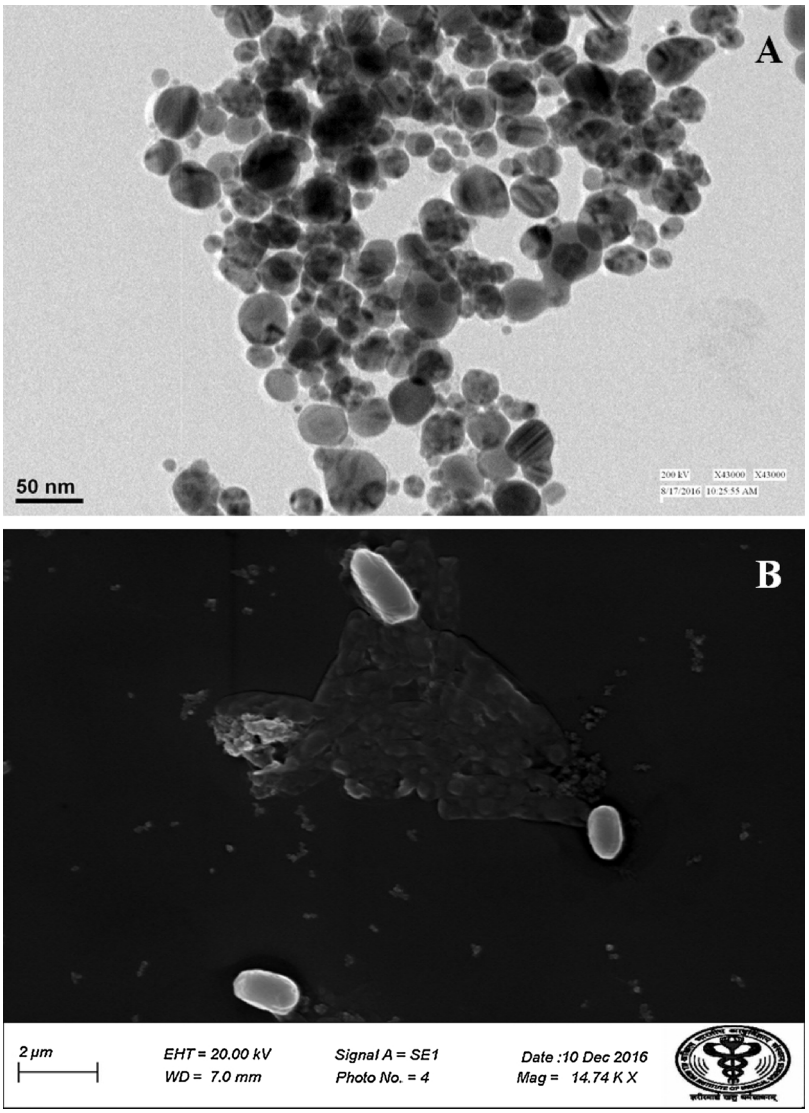

Fig. 2. Identification of Morphological characters of AgNPs **(A)** TEM micrograph, and **(B)** SEM micrograph of biosynthesized AgNPs.

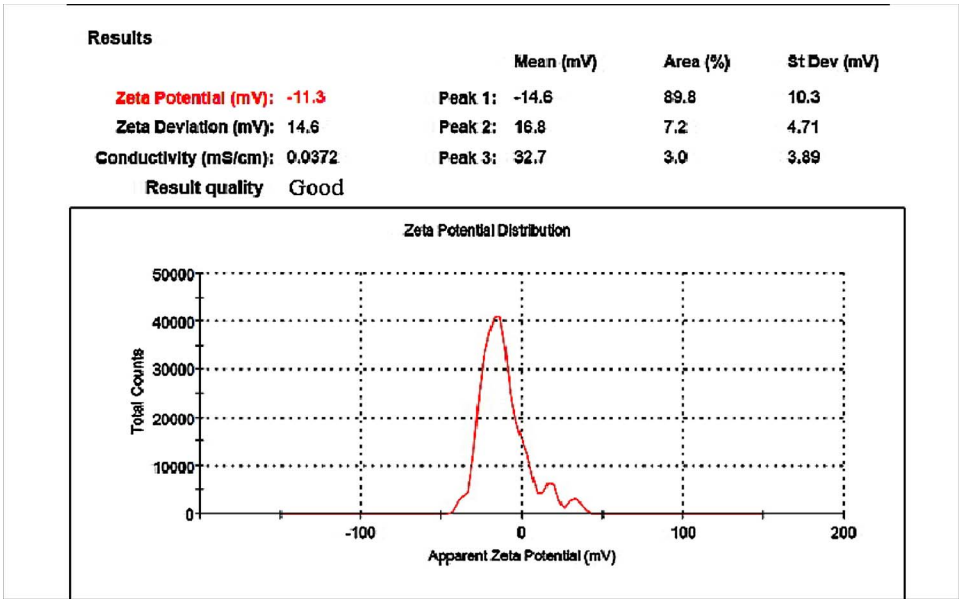

Fig. 3. Zeta potential of biosynthesized AgNPs.

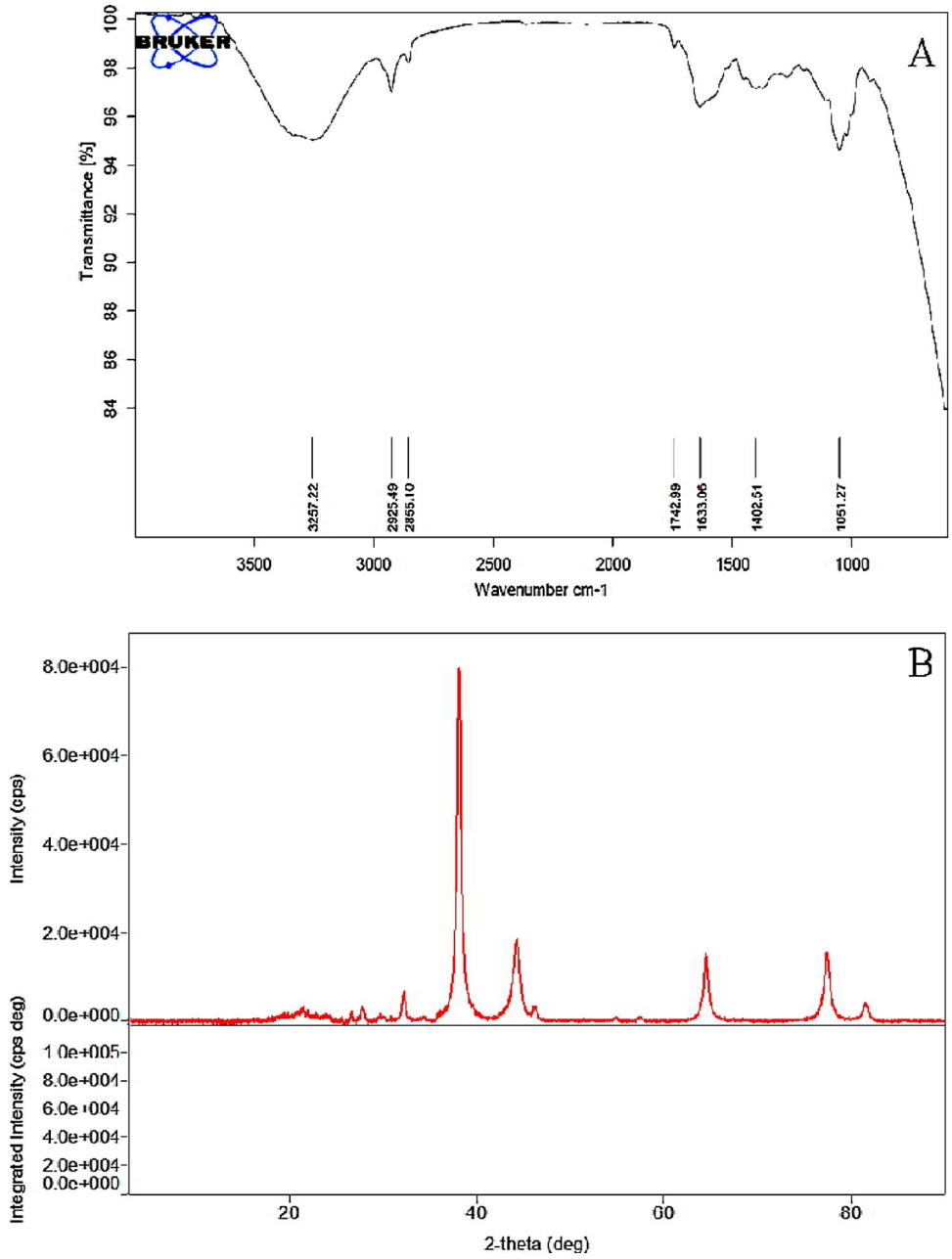

Fig. 4. Depiction of functional groups on AgNPs **(A)** FT-IR spectrum and **(B)** X-ray diffraction pattern.

dose-dependent manner, but significant recoupment was shown by AgNPs at a dose of 100 µg/kg. AgNPs and silymarin restored the elevated levels of liver markers significantly ($P \leq 0.05$) towards normal. Percent protection revealed that AgNPs at 100 µg/kg, dose showed more recovery.

3.5. Determination of tissues biochemical assay

Table 2 depicts the effect of NDEA and synthetic drug (AgNPs) on hepatic tissues. Reduced glutathione levels (GSH) were significantly depleted in NDEA induced rats compared to saline-treated control group whereas oxidized glutathione level (GSSG) was significantly increased ($P \leq 0.05$). AgNPs prevented the depletion of reduced glutathione content and significantly restored the GSSG content ($P \leq 0.05$). All doses were found effective but the significant retrieval was found with AgNPs at a dose of 100 µg/kg which was nearly equal to the recoupment shown by the standard hepatoprotective drug. The current study showed a decline in the activities of G-6-Pase and ATPase in NDEA administered animals. Treatment with AgNPs was found to be effective in restoring these enzymatic parameters in a dose-dependent manner. 100 µg/kg dose of AgNPs showed maximum recovery in these enzyme activities in experimental animals.

3.6. Histopathological observations

Unfortunately, the various morphologic appearances of the hepatic ailments can be difficult to distinguish individually. It is, therefore, very important to correlate clinical information with the pathologic findings. As shown in (Fig. 6A), the cell plate from the hepatic tissue of the control group have intact structure and the boundary between cells was clear. Hepatocytes showed normal structure (H) with a prominent nucleus (N), clear central vein (CV) and well-formed sinusoidal spaces (SS). Exposure of NDEA caused extensive hepatic necrosis (HN) and arrow indicate inflammatory infiltrate with abnormal hepatocellular

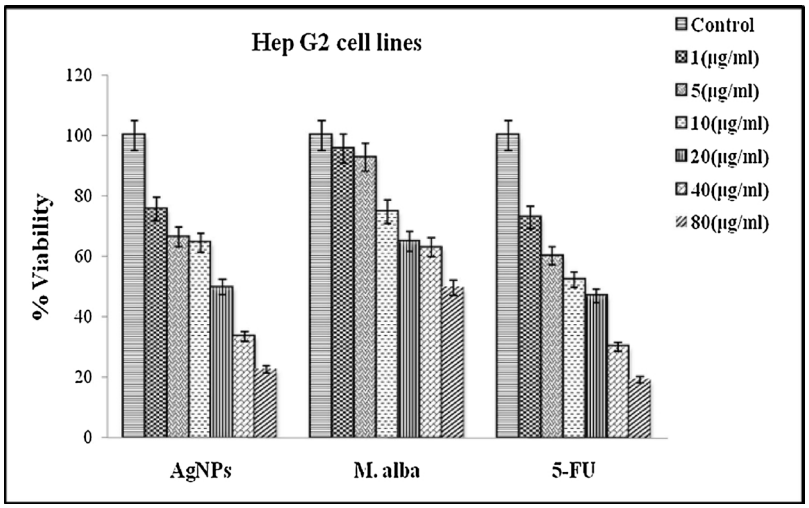

Fig. 5. Dose-dependent cytotoxicity (MTT assay) of AgNPs and *M.alba* extract against liver cancer cells with 24 h treatment compared with the standard anticancer drug (5-FU). Abbreviation: MTT, 3-(4,5-dimethylthiazol-2yl)-2,5-diphenyl tetrazolium; AgNPs, Silver nanoparticles; *M.alba*, *Morus alba*; 5-FU, 5-Fluorouracil. Values are mean ± SD; N = 3; $p < 0.05$ *versus* untreated control.

histology, prominent hyperbasophilic preneoplastic focal lesions and eosinophilic clear cell foci, degenerated tumor cells, as suggested by cell enlargement and distorted hepatic cord and nuclear dissolution (Fig. 6B). Therapy with AgNPs at a dose of 25 µg/kg showed slight recovery and regeneration of some hepatocytes, preserved architecture with mild portal inflammation, mild dysplastic nuclei and dilation in sinusoidal spaces (DSS) still persists (Fig. 6C). Treatment of AgNPs at 50 and 100 µg/kg doses showed a normal lobular pattern with well-formed polygonal hepatocytes (H), having a conspicuous nucleus (N), and wider sinusoidal spaces (S) (Fig. 6D-E). In silymarin (50 mg/kg) treated group hepatic tissues have almost regained their normal pattern and showed well preserved hexagonal hepatocytes (H) with prominent nuclei (N) (Fig. 6F).

4. Discussion

Various plant-based drug has been found to restrain tumor growth and cause a phenotype reversion in certain cancers. Natural drugs have received much attention as sources of biologically active substances including antioxidants, antimutagens and anticarcinogens [40]. These natural drugs give little hope for the restoration of health because of their non targeted action and slow absorption as well as few of the drugs are less effective and show long-term recovery. Recently, biodegradable nanoparticles have been frequently used as drug delivery vehicles due to its splendid bioavailability, better encapsulation and drug targeted efficacy. The present study was aimed to synthesize the silver nanoparticles by *M. alba* leaves and to determine their antiproliferative effect against HepG2 cells and hepatocellular recovery against NDEA induced toxicity in a rat model.

When an aqueous extract of *M. alba* was mixed with silver nitrate, it starts to change the color from colorless to dark brown due to the reduction process of silver ions [41]. The appearance of a dark brown color was the primary indication of the formation of silver nanoparticles. Color change spectrum band of the corresponding temperature confirmed the maximum synthesis at 90°C when compared to below and higher temperature and incubation. Ahmed et al. [22] applied a rapid and simple approach for the synthesis of silver nanoparticles using *Azadirachta indica* aqueous leaf extract, thus are in

Table 2
Protective effect of AgNPs on NDEA induced alterations in tissue biochemistry

Treatments	GSH (U/L)	GSSG (U/L)	G-6-Pase(mg Pi/100 ml/min)	ATPase (µmole Pi/min/g liver)
Control	7.6 ± 0.39	3.67 ± 0.20	6.80 ± 0.37	1971 ± 108
AgNPs *per se*	7.4 ± 0.40	3.92 ± 0.21	5.57 ± 0.30	1970 ± 108
NDEA *per se*	4.6 ± 0.25[a]	18.9 ± 1.04[a]	3.14 ± 0.17[a]	849.0 ± 46.9[a]
NDEA + AgNPs 25 µg/kg	6.5 ± 0.35[*]	12.8 ± 0.71[*]	4.08 ± 0.22[*]	1242 ± 68.6[*]
NDEA + AgNPs 50 µg/kg	6.8 ± 0.38[*]	8.59 ± 0.47[*]	4.71 ± 0.26[*]	1350 ± 74.6[*]
NDEA + AgNPs 100 µg/kg	7.2 ± 0.38[*]	5.20 ± 0.28[*]	5.32 ± 0.29[*]	1560 ± 86.2[*]
NDEA + Sily 50 mg/kg	7.3 ± 0.39[*]	4.48 ± 0.24[*]	5.42 ± 0.29[*]	1650 ± 91.2[*]

Abbreviation: NDEA, *N*-nitrosodiethylamine; AgNPs, Silver nanoparticles; Sily, Silymarin; GSH, Reduced glutathione; GSSG, Oxidised glutathione; G-6-Pase, Glucose-6-Phosphatase; ATPase, Adenosine triphosphatase.
[@] Significant at 5% for ANOVA.
[a] NDEA vs Control.
[*] NDEA+ Therapy vs NDEA at P ≤ 0.05.

Table 1
Therapeutic effect of AgNPs on LFTs biomarker against NDEA intoxication.

Treatments	ALT (U/L)	ALP (U/L)	Albumin(g/dl)	T. Bilirubin (mg/dl)	γ-GT(U/L)
Control	46.7 ± 2.5	178 ± 9.84	3.4 ± 0.18	0.26 ± 0.01	6.2 ± 0.34
AgNPs *per se*	46.0 ± 2.5	180 ± 9.95	3.5 ± 0.19	0.27 ± 0.01	6.0 ± 0.33
NDEA *per se*	210 ± 11.6[a]	326 ± 18.0[a]	1.8 ± 0.09[a]	2.01 ± 0.11[a]	19 ± 1.06[a]
NDEA + AgNPs 25 µg/kg	98.4 ± 5.4[*]	198 ± 10.9[*]	3.0 ± 0.16[*]	1.50 ± 0.08[*]	13 ± 0.72[*]
NDEA + AgNPs 50 µg/kg	69.5 ± 3.8[*]	188 ± 10.4[*]	3.2 ± 0.17[*]	0.72 ± 0.03[*]	9.6 ± 0.53[*]
NDEA + AgNPs 100 µg/kg	56.8 ± 3.1[*]	186 ± 10.3[*]	3.3 ± 0.18[*]	0.32 ± 0.01[*]	7.0 ± 0.38[*]
NDEA + Sily 50 mg/kg	48.2 ± 2.6[*]	179 ± 9.90[*]	3.5 ± 0.19[*]	0.29 ± 0.01[*]	6.8 ± 0.37[*]

Abbreviation: NDEA, *N*-nitrosodiethylamine; AgNPs, Silver nanoparticles; Sily, Silymarin; ALT, Alanine aminotransferase. ALP, Alkaline phosphatase; γ-GT, Gamma-glutamyl transpeptidase.
[@] Significant at 5% for ANOVA.
[a] NDEA vs Control.
[*] NDEA+ Therapy vs NDEA at P ≤ 0.05.

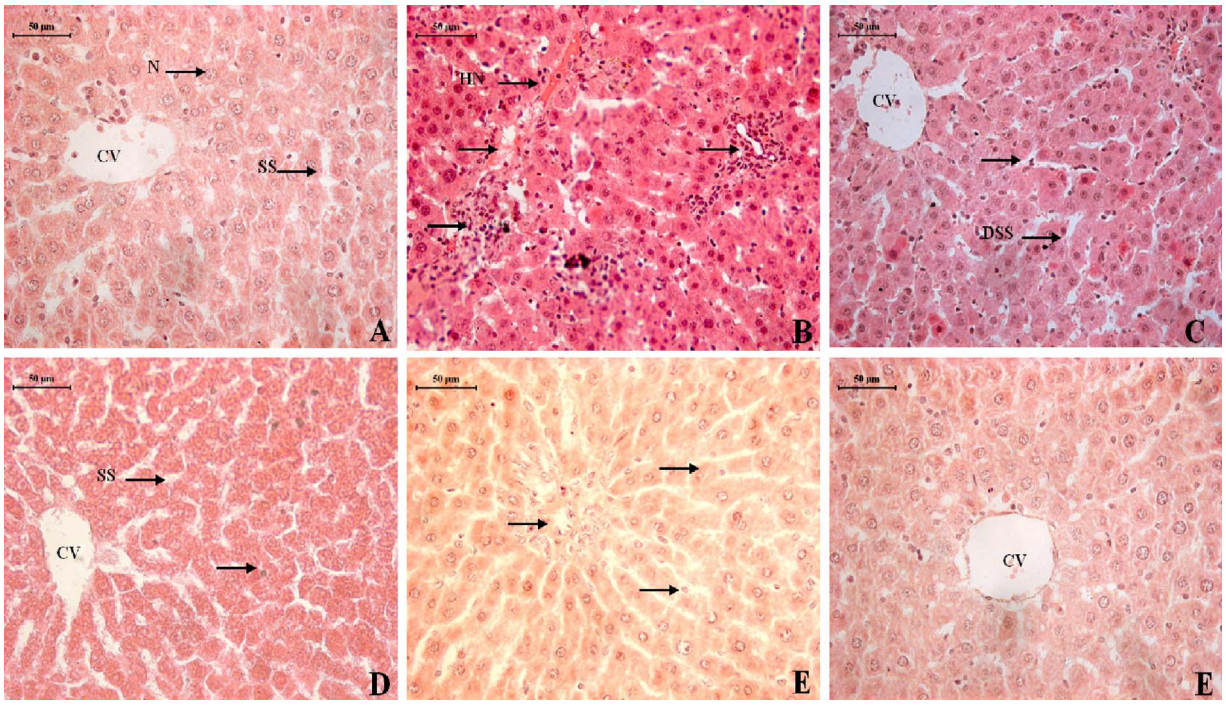

Fig. 6. Photomicrographs of rat liver sections in the different experimental groups showing effect of NDEA and its subsequent treatment with different doses of AgNPS. **A:** Liver sections of control group, **B:** Liver of rat treated with NDEA, **C:** Liver of rat treated with AgNPs (25 µg/kg) after NDEA intoxication, **D–E:** Liver of rat treated with AgNPs (50 & 100 µg/kg) after NDEA intoxication, **F:** Liver of rat treated with Silymarin (50 mg/kg) after NDEA intoxication.

conformity with the current studies. This study proved that the synthesis of nanoparticles increased with increase in temperature, same was reported by earlier researchers [42]. The synthesized AgNPs showed remarkable optical properties which were confirmed by the UV–visible spectra at 410 nm due to the excitation of surface plasma resonance (SPR) [21]. An earlier report has predicted that the SPR in the region around 390–420 nm can be recognized to spherical nanoparticles with a size range from 10 to 50 nm [43,44]. The average particle size was determined by TEM analysis and it was found to be below 50 nm as revealed in the size distribution plate. The SEM and TEM images showed the spherical shape of AgNPs with the size range below 50 nm. These results were also similar with results of Kalimuthu et al. [45].

The FTIR spectrum of AgNPs showed strong absorption peak at 3836 cm^{-1}, 2924 cm^{-1}, 1560 cm^{-1}, 1455 cm^{-1}, 1045 cm^{-1} and 699 cm^{-1} which depict the variety of functional groups such as flavonoids, phenolic and triterpenoids in the leaf extract, which may possibly influence the reduction and stabilization of silver nanoparticles. These results were similar to the reports of Dubey et al. and Suriyakalaaa et al. [46,21]. Recently, Phyto-compounds have been explored to serve mankind in various aspects, the interaction between plant biochemicals and inorganic nanoparticles tend to be a hopeful area in nanoscience and technology [47]. Zeta potential analysis showed the surface charge of particles and revealed a value of −11.3 mV indicating its stability. The negative value indicated the stability of the nanoparticles and it evaded the agglomeration of nanoparticles [48]. The negative potential value might be due to the capping action of biomolecules present in the leaf of *M. alba.* There are many more methods to find out the stability of nanoparticles like sedimentation method, centrifugation method, spectral absorbance analysis and use of surfactants [49–51]. XRD patterns of nanoparticles exhibit several size-dependent features leading to peak position, heights and widths. In the present study, sharp peaks were observed other than the silver region. These might have resulted from the bio-organic compounds in the *M. alba.* The obtained result showed crystalline nature of AgNPs which was supported by the results stated by Shankar et al. [52].

Despite the extensive use of synthetic AgNPs, there are only a few studies to determine the anticancer potential of biologically synthesized AgNPs, particularly in the context of programmed cell death. Nanomedicine has the potential to modernize cancer therapy [53]. The cytotoxicity of biosynthesized AgNPs against HepG2 cells was confirmed by the MTT assay. This was the first study to report the cytotoxicity of *M. alba* mediated AgNPs against hepatocellular carcinoma (HepG2) cell lines. This study investigated that the induction of apoptosis could be the possible mechanism for antiproliferative activity of biosynthesized AgNPs. The AgNPs enter the cancer cells, they interact with the cellular materials, cause DNA damage and cell death. The dose-dependent cytotoxicity was observed in AgNPs treated HepG2 cells. The 50% of cell death was observed at the dose of 20 µg/mL for AgNPs and 80 µg/mL for *M. alba* extract, which determine the inhibitory concentration (IC_{50}) value of both the drugs. Similar reports regarding cytotoxicity were discussed by Fathy et al. [54]. The cytotoxic effect was compared with the standard anticancer drug 5-FU against HepG2 cells and their IC_{50} value was observed at 30 µg/mL. The effect of biosynthesized AgNPs and 5-FU exhibit significant cytotoxicity as compared to *M. alba* extract. A large number of *in vitro* studies indicated that natural drugs inhibit the proliferation of cancerous cells. Zeng et al. [55] investigated the potential of optical nanoparticles for diagnosis and treatment of human diseases and found that they provide uniform information when applied as probes in biological and medical fields. Indeed our result provides most significantly conclusive evidence for the cytotoxic effect of biosynthesized AgNPs against HepG2 cells compared with the crude extract of *M. alba.* This may be due to the presence of small size and phenolic compounds as functional groups on AgNPs.

In the present study, targeted drug delivery of the biologically synthesized silver nanoparticles as nanomedicine effectively recouped the biochemical and histopathological alteration inflicted by the toxicant. Nanoparticles as drug delivery systems are intended to improve the pharmacological and therapeutic potential of conventional drugs. Nanoparticles are capable to penetrate tissues, going through the fenestration of the blood-vessel epithelial tissue as has been validated by

Li et al. [56]. They can enter the systemic blood circulation without forming blood platelet aggregates due to their reduced particle size, provide high surface area and hence a strategy for faster drug release. Rats were selected as the *in vivo* model of exposure because of their similarity with human metabolic, biochemical and physiological pathways [57].

A significant increase of marker enzymes in serum is an indication of damage in the liver plasma membrane, due to the oxidation of polyunsaturated fatty acids in the plasma membrane by ROS generated by the metabolism of NDEA [58]. Exposure of rat to NDEA showed hepatic damage, as was indicated by the increase in the level of ALT, ALP, γ-GT and bilirubin with a concomitant reduction in albumin level. An elevated level of serum indices of hepatocellular damages has been previously reported in many models of NDEA induced hepatocellular degeneration [59]. The current result showed that the exposure of rats to NDEA along with the dose of fabricated AgNPs restored the level of these enzymes. The reversal of increased serum enzymes in NDEA- induced hepatic damage by the AgNPs may be due to the prevention of the leakage of intracellular enzymes by its membrane stabilizing activity. This is an agreement with the commonly accepted view that serum levels of LFTs biomarkers return to normal with the healing of hepatic parenchyma and the regeneration of hepatocytes [60].

The first line of a defense system for oxidative stress is glutathione which gets depleted in the toxicant-induced group indicates the cellular damage. Such cellular damage was revived in the treatment groups. Current results were consistent with previous findings [61]. Pradeep et al. [32] reported a subsequent decrease in the antioxidant defense due to decreased expression of antioxidants during hepatocellular damages. Current results were in line with the findings of Karthikeyan et al. [61] were levels of GSH depleted in the toxicant-induced animals and showed the cellular damage. The revival of GSH and GSSG in treatment groups may possibly determine the regression of injuries to the liver. Explanations of the possible mechanism underlying the hepatoprotective properties of drugs include the prevention of GSH depletion and destruction of free radicals [55].

ATPase activity may be considered as a marker for assessing hepatocellular damage induced by hepatotoxic agents. Pathological processes that interfere with the production of ATP may interfere with sodium pump activity, which in turn results in decreased hepatocellular function. It has been hypothesized that oxidative damage of membrane-bound ATPase activity is crucial for mitochondrial membrane damage [62]. This study showed a significant depletion in the enzymatic activity of ATPase after NDEA intoxication, which was responsible for the impaired function of the respiratory chain and metabolism of ATP. G-6-Pase is a crucial enzyme of glucose homeostasis and plays an important role in the regulation of the blood glucose level. Cellular membrane damage leads to decrease the activity of endoplasmic reticulum such as G-6-Pase [63]. After NDEA exposure significant depletion was observed in G-6-Pase activity in hepatic tissues which might be due to the membrane fragility and permeability of liver. Therapy of AgNPs at all doses significantly restored the metabolic enzyme activities which indicate the improved the physiological functioning of hepatic tissues. Chitosan nanoparticles in combination with quercetin have been reported as a promising candidate as drug delivery, enhances the curative effect of quercetin against the cytogenetic effect of aflatoxin B_1 (AFB_1), thus supports the current findings [64].

Histopathological observation also provided compassionate proof for the enzyme level returns to normal with the healing of hepatic parenchyma and regeneration of hepatocytes. These histological appearances have nearly returned to normal by therapy with nano-drug. The morphological changes observed in current work were comparable to the previously reported data of earlier researchers who also mentioned that NPs recovered the histopathological alterations [65].

5. Conclusion

The present study documented first ever synthesis and characterization of AgNPs using *M. alba* leaf extract. Such biologically synthesized AgNPs possess superior cytotoxic and hepatoprotective activity as compared to a crude extract of *M. alba*. Thus it can be concluded that the compounds of *M. alba* leaves which were attached as functional groups to AgNPs would exert a therapeutic potential and AgNPs enhance their efficacy by reversing the oxidant-antioxidant imbalance during hepatotoxicity induced by NDEA. Thus based on our findings, we suggest that biologically synthesized nanoscale silver particles could be used to treat hepatocellular ailments. There is a wide scope for detailed investigation to elucidate the specific molecular mechanism involved in cell growth inhibition so that they can be used in the future as chemopreventive or therapeutic agents.

Conflict of interests

The authors declare no conflicts of interest in this work.

Acknowledgments

Authors are thankful to Jiwaji University, Gwalior (M.P.) for laboratory facilities and University Grants Commission (UGC) New Delhi for providing the financial assistance under UGC Research Fellowship in Science for Meritorious Students Scheme (Fellowship No. 25- 1/2014-15/(BSR)/7-97/2007(BSR) 25 Aug 2015) to Asha Singh.

References

[1] D.V. Kulkarni, P.S. Kulkarni, Green synthesis of copper nanoparticles using *Ocimum sanctum* leaf extract, Int. J. Chem. Stud. 1 (3) (2013) 2321–4902.
[2] A. Umer, S. Naveed, N. Ramzan, Selection of a suitable method for the synthesis of copper nanoparticles, Nano: Brief Rep. Rev. 7 (5) (2012) 1230005–1230020.
[3] A. Bhatia, P. Shard, D. Chopra, T. Mishra, Chitosan nanoparticles as carrier of immunorestoratory plant extract: synthesis, characterization and immunorestoratory efficacy, Int. J. Drug Deliv. 3 (2011) 381–385.
[4] D.A. LaVan, T. McGuire, R. Langer, Small-scale systems for *in vivo* drug delivery, Nat. Biotechnol. 21 (2003) 1184–1191.
[5] A. Cavalcanti, B. Shirinzadeh, R.A. Freitas, T. Hogg, Nanorobot architecture for medical target identification, Nanotechnology 19 (1) (2008) 015103.
[6] P.K. Jain, X. Huang, I.H. El-Sayed, M.A. El-Sayed, Noble metals on the nanoscale: optical and photothermal properties and some applications in imaging, sensing, biology, and medicine, Acc. Chem. Res. 41 (2008) 1578–1586.
[7] S. Prakash, S. Vidyadhara, R.L.C. Sasidhar, D. Abhijit, D. Akhilesh, Nanonization: a novel approach for enhancement of bioavailability of poorly soluble drugs, J. Nanopharm. Drug Deliv. 1 (3) (2013) 227–239.
[8] D.E. Coricovac, E.A. Moaca, L. Pinzaru, C. Citu, C. Soica, C.V. Mihali, C. Pacurariu, V.A. Tutelyan, A. Tsatsakis, C.A. Dehelean, Biocompatible colloidal suspensios based on magnetic iron oxide nanoparticles: synthesis characterization and toxicological profile, Front. Pharmacol. 8 (2017) 1–18.
[9] O. Lieleg, R.M. Baumgartel, A.R. Bausch, Selective filtering of particles by the extracellular matrix: an electrostatic bandpass, Biophys. J. 97 (2009) 1569–1577.
[10] A.B. Engin, D. Nikitovic, M. Neagu, P.H. Noak, A.O. Docea, M.I. Shtilman, K. Golokhvast, A.M. Tsatsakis, Mechanistic understanding of nanoparticles interactions with extracellular matrix: the cell and immune system, Part. Fibre Toxicol. 14 (22) (2016) 1–16.
[11] S. Poulose, T. Panda, P.P. Nair, T. Théodore, Biosynthesis of silver nanoparticles, J. Nanosci. Nanotechnol. 14 (2014) 2038–2049.
[12] V.V. Makarov, A.J. Love, O.V. Sinitsyna, S.S. Makarova, I.V. Yaminsky, M.E. Taliansky, N.O. Kalinina, Green nanotechnologies: synthesis of metal nanoparticles using plants, Acta Nat. 6 (2014) 35–44.
[13] K.B. Narayanan, N. Sakthivel, Biological synthesis of metal nanoparticles by microbes, Adv. Colloid Interface Sci. 156 (2010) 1–13.
[14] A.K. Mittal, Y. Chisti, U.C. Banerjee, Synthesis of metallic nanoparticles using plant extracts, Biotechnol. Adv. 31 (2013) 346–356.
[15] S.A. Dahoumane, C. Yepremian, C. Djediat, A. Coute, F. Fievet, T. Coradin, R. Brayner, A global approach of the mechanism involved in the biosynthesis of gold colloids using micro-algae, J. Nanopart. Res. 16 (2014) 2607.
[16] J.J. Antony, M.A.A. Sithika, T.A. Joseph, U. Suriyakalaa, A. Sankarganesh, D. Siva, S. Kalaiselvi, S. Achiraman, *In vivo* antitumor activity of biosynthesized silver nanoparticles using Ficus religiosa as a nanofactory in DAL induced mice model, Colloids Surf. B Biointerfaces 108 (2013) 185–190.
[17] K.D. Arunachalam, L.B. Arun, S.K. Annamalai, A.M. Arunachalam, Biofunctionalized gold nanoparticles synthesis from gymnema sylvestre and its preliminary anticancer activity, Int. J. Pharm. Pharm. Sci. 6 (2014) 423–430.

[18] F.S. Rosarin, V. Arulmozhi, S. Nagarajan, S. Mirunalini, Antiproliferative effect of silver nanoparticles synthesized using amla on Hep2 cell line, Asian Pac. J. Trop. Med. 6 (1) (2013) 1–10.

[19] R. Sukirtha, K.M. Priyanka, J.J. Antony, S. Kamalakkannan, R. Thangam, P. Gunasekaran, M. Krishnan, S. Achiramana, Cytotoxic effect of Green synthesized silver nanoparticles using Melia azedarach against in vitro HeLa cell lines and lymphoma mice model, Process Biochem. 47 (2012) 273–279.

[20] U. Suriyakalaa, J.J. Antonya, S. Suganya, Durairaj Siva, Raman Sukirtha, S. Kamalakkannan, P.B.T. Pichiah, S. Achiraman, Hepatocurative activity of biosynthesized silver nanoparticles fabricated using Andrographis paniculata, Colloids Surf. B Biointerfaces 102 (2013) 189–194.

[21] M. Sathishkumar, K. Sneha, S.W. Won, C.W. Cho, S. Kim, Y.S. Yun, Cinnamon zeylanicum bark extract and powder mediated green synthesis of nano-crystalline silver particles and its bactericidal activity, Colloids Surf. B Biointerfaces 73 (2009) 332–338.

[22] S. Ahmed, M. Ahmad, B.L. Swami, S. Ikram, Green synthesis of silver nanoparticles using Azadirachta indica aqueous leaf extract, J. Radiat. Res. Appl. Sci. 9 (1) (2016) 1–7.

[23] W. Tang, G. Eisenbrand, Handbook of Chinese Medicinal Plants: Chemistry, Pharmacology, Toxicology vol. 1, Wiley-VCHWeinheim, 2011, pp. 246–249.

[24] K. Doi, T. Kojima, M. Makino, Y. Kimura, Y. Fujimoto, Studies on the constituents of the leaves of *Morus alba* L, Chem. Pharm. Bull 49 (2001) 151–153.

[25] Y. Qian, C.Q. Ling, Preventive effect of Ganfujian granule on experimental hepatocarcinoma in rats, World J. Gastroenterol. 10 (2004) 755–757.

[26] R. Misra, S. Acharya, S.K. Sahoo, Cancer nanotechnology: application of nanotechnology in cancer therapy, Drug Discov. Today 15 (2010) 842–850.

[27] O.B. Oloyede, T.O. Ajiboye, Y.O. Komolafe, N nitrosodiethylamine induced redox imbalance in rat liver: protective role of polyphenolic extract of *Blighia sapida arilli*, Free Radic. Antioxid. 3 (2013) 25–29.

[28] S. Preston-Martin, R. Munir, R. Chakrabarti Reema, Nervous system, in: David Schottenfeld, Joseph F. Fraumeni (Eds.), Cancer Epidemiology and Prevention, oxford University Press, New York, 2006, pp. 1173–1195.

[29] M. Dietrich, G. Block, J.M. Pogoda, P. Buffler, S. Hecht, S. Preston-Martin, A review: dietary and endogenously formed N-nitroso compounds and risks of childhood brain tumours, Cancer Causes Control 16 (2005) 619–635.

[30] W. Hai, C. Kim, S. Song, C. Kang, Study on mechanism of multistep hepato tumorigenesis in rat: development of hepatotumorigenesis, J. Vet. Sci. 2 (2001) 53–58.

[31] S.K. Hassan, A.M. Mousa, M.G. Eshak, A.E.R.H. Farrag, A.E.F.M. Badawi, Therapeutic and chemopreventive effects of nano curcumin against diethylnitrosamine induced hepatocellular carcinoma in rats, Int. J. Pharm. Pharm. Sci. 6 (3) (2014) 54–62.

[32] K. Pradeep, C.V.R. Mohan, K. Gobianand, S. Karthikeyan, Silymarin modulates the oxidant-antioxidant imbalance during diethylnitrosamine-induced oxidative stress in rats, Eur. J. Pharm. 560 (2007) 110–116.

[33] U. Suriyakalaaa, J.J. Antonya, S. Suganyaa, D. Sivaa, Hepatocurative activity of biosynthesized silver nanoparticles fabricated using *Andrographis paniculata*, Colloids Surf. B Biointerfaces 102 (2013) 189–194.

[34] M.B. Hansen, S.E. Nielsen, K. Berg, Re-examination and further development of a precise and rapid dye method for measuring cell growth/cell kill, J. Immunol. Methods 119 (1989) 203–210.

[35] D. Liu, L. Zhi, M. Ma, D. Qiao, M. Wang, Y. Wang, B. Jin, A. Li, G. Liu, Y. Zhang, Y. Song, H. Zhang, Primarily screening and analyzing ESTs differentially expressed in rats' primary liver cancer, Chin. J. Cancer Res. 25 (2013) 71–78.

[36] K.K. Anand, B. Singh, A.K. Saxena, B.K. Chandan, V.N. Gupta, V. Bhardwaj, 3, 4, 5-Trihydroxy benzoic acid (gallic acid), the hepatoprotective principle in the fruits of *Terminalia belerica* bioassay guided activity, Pharm. Res. 36 (1997) 315–321.

[37] P.J. Hissin, R. Hilf, A fluorometric method for determination of oxidized and reduced glutathione in tissues, Anal. Biochem. 74 (1976) 214–226.

[38] P.K. Seth, K.K. Tangri, Biochemical effects of some newer salicylic acid congeners, J. Pharm. Pharmacol. 18 (12) (1966) 831–833.

[39] E.S. Baginski, P.F. Piero, Z. Bennie, Methods of Enzymatic Analysis vol. 2, Academic Press, HU Bergmeyer New York, 1974, p. 876.

[40] C.J. Dillard, J.B. German, Phytochemicals, nutraceuticals and human health, J. Sci. Food Agric. 80 (2010) 1744–1756.

[41] S.C. Yang, T.I. Chen, K.Y. Li, T.C. Tsai, Change in phenolic compound content, reductive capacity and ACE inhibitor activity in noni juice during traditional fermentation, J. Food Drug Anal. 15 (2008) 290–298.

[42] R. Sukirthaa, P.K. Manasa, J.J. Antonya, S. Kamalakkannana, R. Thangamb, P. Gunasekaranb, K. Muthukalingan, A. Shanmugam, Cytotoxic effect of Green synthesized silver nanoparticles using *Melia azedarach* against *in vitro* HeLa cell lines and lymphoma mice model, Process Biochem. 47 (2012) 273–279.

[43] A. Panacek, L. Kvitek, R. Prucek, M. Kolar, R. Vecerova, N. Pizurova, V.K. Sharma, T. Nevecna, R. Zboril, Silver colloid nanoparticles: synthesis, characterization and their antibacterial activity, J. Phys. Chem. B 110 (2006) 16248.

[44] Z. Zaheer, Rafiuddin, Silver nanoparticles to self-assembled films: green synthesis and characterization, Colloids Surf. B Biointerfaces 90 (2012) 48.

[45] K. Kalimuthu, R.S. Babu, D. Venkataraman, M. Bilal, S. Gurunathan, Biosynthesis of silver nanocrystals by *Bacillus licheniformis*, Colloids Surf. B Biointerfaces 65 (2008) 150–153.

[46] S.P. Dubey, M. Lahtinen, M. Sillanpaa, Tansy fruit mediated greener synthesis of silver and gold nanoparticles, Process Biochem. 45 (2010) 1065–1071.

[47] A.K. Jhaa, K. Prasad, K. Prasad, A.R. Kulkarni, Plant system: nature's nanofactory, Colloids Surf. B Biointerfaces 73 (2009) 219–223.

[48] S.V. Patil, H.P. Borase, C.D. Patil, B.K. Salunke, Biosynthesis of silver nanoparticles using latex from few euphorbian plants and their antimicrobial potential, Appl. Biochem. Biotechnol. 167 (2012) 776–790.

[49] Y. Li, J. Zhou, S. Tung, E. Schneider, S. Xi, A review on development of nanofluid preparation and characterization, Powder Technol. 196 (2) (2009) 89–101.

[50] H. Zhu, C. Zhang, Y. Tang, J. Wang, B. Ren, Y. Yin, Preparation and thermal conductivity of suspensions of graphite nanoparticles, Carbon 45 (1) (2007) 226–228.

[51] J. Huang, X. Wang, Q. Long, X. Wen, Y. Zhou, L. Li, Influence of pH on the stability characteristics of nanofluids, Proceedings of the Symposium on Photonics and Optoelectronics (SOPO '09) (2009).

[52] S.S. Shankar, A. Ahmad, R. Pasricha, M. Sastry, Bioreduction of chloroaurate ions by geranium leaves and its endophytic fungus yields gold nanoparticles of different shapes, J. Mater. Chem. 13 (2003) 1822.

[53] J.S. Rink, M.P. Plebanek, S. Tripathy, C.S. Thaxton, Update on current and potential nanoparticle cancer therapies, Curr. Opin. Oncol. 25 (6) (2013) 646–651.

[54] S.A. Fathy, A.N. Singab, S.A. Agwa, D.M. Abd El Hamid, F.A. Zahra, S.M. Abd El Moneim, The antiproliferative effect of mulberry (*Morus alba* L.) plant on hepatocarcinoma cell line HepG2, Egypt J. Med. Hum. Genetics 14 (2013) 375–382.

[55] Q. Zeng, D. Shao, W. Ji, J. Li, L. Chen, J. Song, The nanotoxicity investigation of optical nanoparticles to cultured cells *in vitro*, Toxicol. Rep. 1 (2014) 137–144.

[56] C. Li, H. Liu, Y. Sun, H. Wang, F. Guo, S. Rao, J. Deng, Y. Zhang, Y. Miao, C. Guo, J. Meng, X. Chen, L. Li, D. Li, H. Xu, H. Wang, B. Li, C. Jiang, PAMAM nanoparticles promote acute lung injury by inducing autophagic cell death through the Akt-TSC2-mTOR signaling pathway, J. Mol. Cell Biol. 1 (1) (2009) 37–45.

[57] C.A. Argmann, J.Y. Edwards, C.G. Sawyez, C.H. O'Neil, R.A. Hegele, J.G. Pickering, M.W. Huff, Regulation of macrophage cholesterol efflux through hydroxymethylglutaryl-CoA reductase inhibition: a role for RhoA in ABCA1-mediated cholesterol efflux, J. Biol. Chem. 280 (2005) 22212–22221.

[58] S.K. Hassan, A.M. Mousa, M.G. Eshak, A.E.R.H. Farrag, A.E.F.M. Badawi, Therapeutic and chemopreventive effects of nano *Curcumin* against diethylnitrosamine induced hepatocellular carcinoma in rats, Int. J. Pharm. Pharm. Sci. 6 (3) (2014) 54–62.

[59] X. Li, C. Liu, C. Blanche, K.Q. Hu, E. Donald, S. Andrew, X.D. Wang, Tumor progression locus 2 ablation suppressed hepatocellular carcinoma development by inhibiting hepatic inflammation and steatosis in mice, J. Exp. Clin. Cancer Res. 34 (2015) 138.

[60] S.S. Al-Rejaie, A.M. Aleisa, A.A. Al-Yahya, S.A. Bakheet, A. Alsheikh, A.G. Fatani, O.A. Al-Shabanah, M.M. Sayed-Ahmed, Progression of diethylnitrosamine-induced hepatic carcinogenesis in carnitine-depleted rats, World J. Gastroenterol. 15 (11) (2009) 1373–1380.

[61] R. Karthikeyan, P. Anantharaman, N. Chidambaram, T. Balasubramanian, S.T. Somasundaram, Padina boergessenii ameliorates carbon tetrachloride-induced nephrotoxicity in Wistar rats, J. King Saud Univ. Sci. 24 (2012) 227–232.

[62] M.D. Brand, G.D. Nicholls, Assessing mitochondrial dysfunction in cells, Biochem. J. 15 (April) (2011) 297–312.

[63] B.K. Chandan, A.K. Sharma, K.K. Anand, *Boerhavia diffusa*: A study of its hepatoprotective activity, J. Ethnopharmacol. 31 (1991) 299–307.

[64] M.A. Abdel-Wahhab, A. Aljawish, A.A. El-Nekeety, S.H. Abdel-Aiezm, H.A. Abdel-Kader, B.H. Rihn, O. Joubert, Chitosan nanoparticles and quercetin modulate gene expression and prevent the genotoxicity of aflatoxin B1 in rat liver, Toxicol. Rep. 2 (2015) 737–747.

[65] M.S. Reshi, S. Shrivastava, A. Jaswal, N. Sinha, C. Uthra, S. Shukla, Gold nanoparticles ameliorate acetaminophen-induced hepato-renal injury in rats, Exp. Toxicol. Pathol. 69 (2017) 231–240.